Thyroid hormone-dependent apoptosis during metamorphosis in Ciona robusta involves both bilaterian-ancestral and vertebrate-derived processes

Nelly Godefroy, Emilie Le Goff, Qiaowei Pan, Stephen Baghdiguian, Melanie Debiais-Thibaud, Camille Martinand-Mari

1 **Thyroid hormone-dependent apoptosis during metamorphosis in *Ciona robusta***

2 **involves both bilaterian-ancestral and vertebrate-derived processes**

3

4 Short title: TH signal and apoptosis in *Ciona* metamorphosis

5

6 Godefroy Nelly [1], Le Goff Emilie [1], Pan Qiaowei [1,2], Baghdiguian Stephen [1], Debiais-Thibaud

7 Mélanie [1] and Martinand-Mari Camille [1,*]

8 [1] ISEM, Université de Montpellier, CNRS, IRD, EPHE, Montpellier, France

9 [2] present address: Faculty of Biology and Medicine, University of Lausanne, Switzerland

10

11 *Corresponding author: Camille Martinand-Mari

12 E-mail address: camille.martinand-mari@umontpellier.fr; ORCID ID: 0000-0002-9909-

13 0071

14 ISEM UMR5554, Université de Montpellier, Place Eugène Bataillon, 34095 Montpellier

15 cedex 5, France

ABSTRACT

Chordate metamorphosis is a postembryonic larva-to-juvenile transition triggered by thyroid hormones and their specific receptors (TR). This crucial developmental event shows a wide morphological diversity among different chordate lineages and is characterized by ecological, morphological, metabolic and behavioral changes that can be drastic. One of the most studied models is the amphibian Xenopus, whose tadpole metamorphosis includes apoptosis-induced tail regression dependent on the thyroid hormone pathway. In an evolutionary context, we used the ascidian model, the extant closest group to vertebrates, in which the swimming larva transforms to a sessile filter-feeding juvenile during metamorphosis, to study the role of thyroid hormones in this transformation. The ascidian metamorphosis is also characterized by an apoptosis-driven tail regression as in Xenopus. However, whether this apoptosis-driven process is dependent on the thyroid hormone has not yet been elucidated.

In this study, we interfered with thyroid hormone signaling during tail regression of the ascidian *Ciona robusta* to investigate whether (i) thyroid hormone is involved in the regulation of developmental apoptosis, and (ii) apoptosis leading to tail regression involves its classical molecular pathways. We described specific gene expression landmarks as well as apoptosis dynamics during larva metamorphosis under thyroid hormone exposure and thyroid hormone inhibition treatments. We provide evidence that *Ciona robusta* metamorphosis involves thyroid hormone-dependent apoptosis, similar to other studied chordates. However, the mode of action of thyroid hormone shows great variation compared to the classically described scheme in chordates, both in thyroid hormone/TR interactions and in the apoptotic pathway.

Key words: metamorphosis, thyroid hormone, post-embryonic development, apoptosis, ascidian, chordate evolution

Abbreviations: T3: tri-iodothyronine; T4: thyroxin; TR: thyroid hormone receptor; TU thiourea; hpf: hours post-fertilization; hph: hours post-hatching.

1. Introduction

The thyroid hormones thyroxin (T4) and its derivative tri-iodothyronine (T3) are essential to organogenesis and tissue rearrangements during metamorphosis, as well as to growth, development, tissue homeostasis and metabolism during the full life cycle of vertebrates (Mullur *et al.*, 2014; Seoane-Collazo *et al.*, 2015; Goemann *et al.*, 2017). Thyroid hormones circulate in the plasma (Roche *et al.*, 1962; Barrington & Thorpe, 1965; Fujita & Sawano, 1979; Dunn, 1980a; b; Di Fiore *et al.*, 1997) and are activated/catalyzed by deiodinases in the tissues (Darras and Van Herck, 2012). Amphibians have been used as a model to study vertebrate metamorphosis for almost a century. Metamorphosis involves the remodeling of several organ systems which necessitates the orchestration of both cell proliferation and cell death: in this regard, one spectacular event in amphibian metamorphosis is tail regression that involves apoptosis in the muscular, skeletal and nervous systems, regulated by thyroid hormone signaling (Sachs *et al.*, 2000a; Shi & Ishizuya-Oka, 2001; Tata, 2006; Ishizuya-Oka, 2011). The molecular mechanisms involved in vertebrate metamorphosis were best described in the studies of amphibians and some teleost fishes. In both models, thyroid hormones function by binding to their nuclear receptors (thyroid hormone receptors, TRα and TRβ) that act as transcription factors to regulate developmental gene expression, including apoptotic genes (for reviews, see Ishizuya-Oka *et al.*, 2010; Grimaldi *et al.*, 2013; Holzer & Laudet, 2013; Morvan-Dubois *et al.*, 2013; Wrutniak-Cabello *et al.*, 2017). TR does not usually bind DNA alone but first forms heterodimers with retinoid X receptor (RXRs: RXRα, RXRβ and RXRγ) and then TR/RXR acts as the functional unit to bind DNA and control gene transcription (Ikeda *et al.*, 1994; Machado *et al.*, 2009). During *Xenopus* tail regression, the thyroid hormone signaling pathway up-regulates *TRβ* expression and down-regulates *RXRγ* expression (Ikeda *et al.*, 1994; Machado *et al.*, 2009).

Despite a quite complete description of cellular events linked to metamorphosis in Xenopus, including the relationship between TH signaling regulating apoptosis wave(s), there has been little data suggesting this observation is generalized to all vertebrates, or may even be shared with more distant groups. Ascidians represent the extant sister-group to vertebrates and are very easily manipulable in laboratory. Metamorphosis of the ascidian *Ciona robusta* (Brunetti *et al.*, 2015) represents a period of profound morphological changes during which the animal alters its life traits (Sasakura & Hozumi,

79   2017). The lecithotrophic larva has a prototypical chordate body plan, it swims a few

80   hours after hatching and before adhering to the substrate, and then needs a few more

81   hours to metamorphose into a sessile filter-feeding juvenile in laboratory conditions

82   (Matsunobu & Sasakura, 2015). The initiation of metamorphosis is sensitive to several

83   internal and external cues and is morphologically first characterized by tail regression

84   (Matsunobu & Sasakura, 2015), which involves apoptosis (Chambon *et al.*, 2002; Tarallo

85   & Sordino, 2004) and cell migration to the trunk region (For review, see Karaiskou *et al.*,

86   2015). To date, whether thyroid hormone plays a conserved role in the regulation of this

87   apoptotic event in ascidians is not known.

88   In *Ciona robusta* adults, the synthesis of thyroid hormones was suggested to take place in

89   the endostyle, an organ homologous to the thyroid gland of vertebrates (Ogasawara *et al.*,

90   1999). While no endostyle nor blood circulatory system has yet developed in the larvae

91   of *Ciona robusta*, T4 is already present in the tail of 24-hour-old larvae (Patricolo *et al.*,

92   2001). In previous studies, *Ciona robusta* larvae were treated with exogenous T4 or

93   thiourea (TU, an inhibitor of thyroid hormone synthesis), which showed that thyroid

94   hormone is involved in the regulation of metamorphosis (Patricolo *et al.*, 2001; D'Agati &

95   Cammarata, 2006). In the genome of *Ciona robusta*, a single TR ortholog was identified.

96   This TR gene contains a highly conserved DNA binding domain, similar to that of

97   vertebrates. The expression of this TR has been detected in the embryo and larva,

98   suggesting a possible role during embryonic development and metamorphosis in *Ciona*

99   *robusta* (Carosa *et al.*, 1998). However, since this receptor was shown to not bind any

100 iodinated tyrosine derivative *in vitro*, the molecular pathways triggered by thyroid

101 hormones to regulated metamorphosis remain elusive (Carosa *et al.*, 1998; Paris *et al.*,

102 2008). In the genome of *Ciona robusta*, a single RXR ortholog was identified (Yagi *et al.*,

103 2003). In this regard, *Ciona robusta* is more similar to other deuterostomes or bilaterians

104 (Howard-Ashby *et al.*, 2006; Huang *et al.*, 2015; Taylor & Heyland, 2018; Li *et al.*, 2020).

105   In this study, we interfered with thyroid hormone signaling during tail regression

106 to characterize whether (i) thyroid hormones are involved in the regulation of apoptosis

107 and (ii) the process of apoptosis involves actors of the classical apoptotic pathways. In

108 order to address these questions, we describe specific gene expression patterns as well

109 as data on apoptosis dynamics during larva metamorphosis under T4 and TU treatments.

110 We provide evidence that thyroid hormone-dependent apoptosis is involved in *Ciona*

111 *robusta* metamorphosis, similar to previous findings in amphibians. However, the mode

4

112   of action of thyroid hormone shows great variation compared to the classically described

113   scheme in chordates, both in thyroid hormone/TR interactions and in the apoptotic

114   pathway.

115

116

2. Material and methods

2.1. Ethical statement

The research described herein was performed on *Ciona robusta*, a marine invertebrate. The study was carried out in strict accordance with European and French legislations (directives 2010/63 and 2016-XIX-120, respectively) for the care and use of animals for scientific purposes (ISEM agreement N°A34-172-042) although *Ciona robusta* is not included in the organisms designated by this legislation. The study did not involve endangered nor protected species.

2.2. Animal husbandry

Adult *Ciona robusta* were collected in the Thau laguna (SMEL of Montpellier University, France) and maintained at 18°C in a tank with circulating seawater and under constant light to allow gametes accumulation. Oocytes were collected from each individual into separate wells and were fertilized with a mixture of sperms obtained from the different individuals after dissection of gonoducts and spermiducts. Just before fertilization, 50 μl of sperm was activated with 1 ml of Tris 50mM in seawater. Three drops of diluted sperm were used to fertilize each pool of oocytes. Fertilized eggs were reared in tissue culture dishes at 18°C in 0,2 mm filtered seawater containing 100 U/ml penicillin, and 0,1 mg/ml streptomycin (30ml/dish). Embryos and larvae were allowed to develop to the desired stage and then collected or used for further experiments.

2.3. Thyroxin, thiourea and caspase inhibitor treatments

Thiourea powder (TU; 16217, Riedel-de Haën) was dissolved directly in seawater to obtain a 500μM working solution. A stock solution of L-thyroxine (T4; T1775, Sigma) was prepared at 1mM in 0,001N NaOH, which was then diluted with seawater to obtain a 100nM working solution.

Just after hatching, swimming larvae (around 100 larvae/kinetic point) were transferred in new tissue culture dishes containing seawater, T4 or TU solutions (30ml/dish) and collected every two hours for 10 hours for qPCR experiments or at 6 and 12h of treatment for rescue experiments (TUNEL staining).

For the tail amputation experiments, the just hatched larvae were anesthetized with MS222 (Sigma-Aldrich, used at 0,8mM final) and 25% of the posterior end of the tails was

150   removed under the binocular with a needle. Afterwards the amputated larvae (50

151   larvae/kinetic point/treatment) were transferred to tissue culture dishes containing

152   seawater (control) or T4 (100nM in seawater) (30ml/dish). At 6 and 12 hours post

153   treatment, state of larvae was evaluated: no-tail larvae *versus* swimming larvae. The

154   resulting graphs are presented in percentage, 100% corresponding to the total of

155   larvae/plate. Then, larvae were collected and fixed for apoptosis detection by TUNEL

156   staining.

157   Caspase-8 inhibitor Z-IETD-FMK and Caspase-9 inhibitor Z-LEHD-FMK were obtained

158   from R&D Systems and were dissolved in dimethyl sulfoxide (DMSO, Sigma) to give a

159   20mM stock solution. Then they were diluted with seawater to obtain a 100μM working

160   solution. At hatching, swimming larvae (100 larvae/condition) were transferred into 24

161   well plate (500 μl solution/well) and reared in DMSO 0,5% in seawater (DMSO used as

162   control) or caspase inhibitor solutions. The number of tail-regressed larvae was counted

163   10h after treatment.

164

165   *2.4. TUNEL staining and indirect immunofluorescence analysis*

166   Larvae were fixed for 20 min with 3,7% formaldehyde in filtered seawater and

167   then permeabilized for 20 min at room temperature with 0,2 % Triton X-100 in TS

168   solution (150 mM NaCl, 25 mM Tris, pH 7.5). TUNEL staining (Roche, *In situ* cell death

169   detection kit, TMR red) was performed according to the manufacturer's instructions. In

170   brief, larvae were incubated in TUNEL reaction mixture (Enzyme solution 10% in Label

171   solution) 1 hour at 37°C in a humidified chamber. Both negative and positive controls of

172   TUNEL staining were performed according to the manufacturer's instructions. For

173   indirect immunofluorescence, T4 thyroid hormone was detected with a rabbit anti-L-

174   thyroxine polyclonal antibody (T-2652, Sigma), and DNA with DAPI (D9542, Sigma).

175   Appropriate   secondary   antibody   was   FITC-conjugated   donkey-anti-rabbit

176   immunoglobulins (Jackson Laboratories). Specimens were analyzed with a Leica TCS-SPE

177   laser confocal microscope (Montpellier RIO Imaging platform, France).

178

179   *2.5. RNA isolation, semi-quantitative RT-PCR and qPCR analysis*

180   For semi-quantitative PCR experiment, fertilized eggs were allowed to develop to

181   the desired stage, collected every 2 hours from fertilization to 28 hours post-fertilization

182   (hpf) (100 individuals/kinetic point) and frozen before RNA extraction.

183   For qPCR experiments, hatched larvae were treated or not with TU and collected every 2

184   hours to 10 hours post-hatching (hph). At the collecting time, and to focus the study on

185   tail regression, only tails of larvae were collected with a needle under the binocular and

186   frozen before RNA extraction. At each time point, a pool of 100 tails was collected.

187   Total RNA was isolated with RNeasy kit according to the supplier's instructions (QIAGEN).

188   70 ng of total RNA were used for cDNA preparation performed by Superscript II reverse

189   transcriptase (Invitrogen) with an oligodT primer, the mixture was incubated for 50 min

190   at 42°C followed by 15 min at 70°C.

191   Semi-quantitative PCR was performed on cDNA from each time point of kinetic (95°C for

192   5 min and then 35 cycles of 95°C for 30s, 53°C for 30s, 72°C for 1 min, completed at 72°C

193   for 10 min) and PCR products were run on 2% agarose gels at 100 Volts during 30 min.

194   PCR products were quantified by Image J gel analysis. Each lane was normalized with the

195   expression of reference gene S26 (Vincent *et al.*, 1993).

196   For quantitative PCR, 1:20 dilution of each cDNA was run in triplicate on a 384-well plate

197   for each primer pair by using thermal cycling parameters: 95°C for 10 min, 95°C for 10s,

198   63°C for 10s, 72°C for 10s (45 cycles) and an additional step 72°C for 10 min performed

199   on a Light Cycler 480 with the SYBR Green I Master kit (Roche) (qPHD UM2/GenomiX

200   Platform, Montpellier - France). Results were normalized with the expression of reference

201   gene S26. Data were analyzed with the Light Cycler 480 software 1.5.1.

202   All the sequences used come from the Aniseed website (www.aniseed.cnrs.fr). We used

203   Primer 3.0 to design all the sets of forward and reverse primers to amplify selected genes

204   listed in table 1.

205

206   *2.6. Statistical analysis*

207   The semi-quantitative PCR and qPCR experiments were repeated three times

208   (three different spawnings) and the inhibitor treatments were repeated twice. The values

209   are the means +/- standard deviation. At each time point, a Student's t-test was performed

210   to validate a difference of expression between control and treatment (significant at

211    $P<0,05$). ANOVA was done (for qPCR only) with expression as the response, and time,

212   treatment and their interaction as predictors (Table 2).

213

3. Results

3.1. An apoptotic wave in tail cells starts after T4 and CrTR *expression decreases.*

The presence of endogenous T4 in the tail of *Ciona robusta* during metamorphosis is detected by immunofluorescence in larvae from hatching (18hpf) to metamorphosis (30hpf). T4 is detectable in all cell-types of the entire tail at hatching, and then gradually disappears from the posterior to the anterior pole of the tail (Figure 1A and supplementary data). No endostyle nor blood circulatory system has yet developed in the larvae and T4 appears diffuse in all tissues of the larva. A massive apoptotic wave is detected through TUNEL staining and first occurs in cells at the posterior extremity of the tail. Then, this death progresses towards the anterior pole together with T4 disappearance, while tail regression has not started yet (25hpf, Figure 1A; see previous results from (Chambon *et al.*, 2002). The expression of the single thyroid-hormone receptor *CrTR* is undetectable before 8hpf. Then it increases to reach its maximum at around hatching (Figure 1B, C), and finally decreases until 28hpf.

3.2. T4 is necessary for the initiation of the apoptotic wave and the tail regression, and modulates CrTR *and* CrRXR *expression*

The role of T4 in the apoptotic wave was investigated by TU treatment experiments. Larvae were raised in medium treated with TU at hatching and collected either after 6h or after 12h of treatment (middle of apoptotic wave *versus* end of the tail regression period, respectively). In control larvae, the presence of TUNEL-positive nuclei is observed in 80% of larval tails at 6hph and complete tail resorption is observed in 70% of larvae at 12hph, with the remaining 30% still swimming. In TU treated larvae, neither apoptotic nuclei nor caudal regression are observed and 100% of the treated larvae are still swimming (entire tail) after 12h of treatment (Figure 2). The suppression of the apoptotic wave in *Ciona robusta* tail induced by TU is partially reversed by a simultaneous treatment with T4: after 6h of co-treatment, about 50% of larvae show a rescued phenotype with apoptotic nuclei in their tail at 6hph and go through tail regression 12h after co-treatment (Figure 2).

To test cell-autonomy in T4-responsive tail cells, and given the progressive posterior-to-anterior initiation of apoptosis, we performed microsurgery to remove the most posterior zone of the tail. The severed larvae completely stop their metamorphosis,

247 and show no TUNEL staining even at 12hph (Figure 3, A and B in comparison with control

248 larva in figure 2). Tail cells therefore do not answer in a cell-autonomous way to T4

249 signaling. When the severed larvae are treated with T4 directly after the microsurgery,

250 the polarized phenomenon of apoptosis is re-initiated at the posterior pole after 6h of

251 treatment, and this metamorphosis process is re-established in 30% of severed larvae at

252 12hph (Figure 3A). This suggests that a signaling center is generated under T4 signaling

253 pathway at the posterior tip of metamorphic larvae.

254 Hatching larvae were treated with TU and tails were collected at different time

255 points from hatching to the end of tail regression for qPCR experiments. *CrTR* expression

256 decreases over time in control tails (> 7-fold decrease), but treatment with TU

257 significantly prolongs and amplifies its expression (Figure 4A). In contrast, after hatching,

258 the expression of *CrRXR* mRNA increases significantly until reaching a maximum at 6hph

259 and lightly decreases at later stages (Figure 4A and Table 2). The increase of *CrRXR* in the

260 tails is slowed down in TU-treated larvae with a significant difference at 6hph compared

261 to the tails of control larvae (Figure 4B and Table 2).

262

263 *3.3. Caspase 8/9 but not Bax nor Bcl-XL expression is modulated by T4 signaling during tail*

264 *regression in* Ciona robusta

265 Apoptotic mechanisms in vertebrates can be initiated by two classical pathways,

266 the intrinsic (initiated by caspase-9) and extrinsic (initiated by caspases 8 and 10)

267 pathways (Ichim & Tait, 2016). Numerous studies in amphibian metamorphosis showed

268 that the caudal regression is under the control of the intrinsic pathway of apoptosis (Sachs

269 *et al.*, 2004; Rowe *et al.*, 2005; Hanada *et al.*, 2013).

270 In *Ciona robusta,* no caspase was specifically linked to the intrinsic or extrinsic

271 pathway (Chambon *et al.*, 2002; Dehal *et al.*, 2002; Terajima *et al.*, 2003; Weill *et al.*, 2005)

272 but one shows protein domains similar to both caspase-8 and -9 (Weill *et al.*, 2005). This

273 CrCasp8/9 displays two DED motifs in the pro-domain and the pentapeptide QACQG in

274 the active site, similar to human Caspases 8 and 10 and shows a p20/p10 domain more

275 similar to that of human Caspase 9 (Figure 5A and Weill et al., 2005). The expression of

276 *CrCasp8/9* increases from hatching to 6hph where it reaches a peak (two-fold increase

277 compared to at hatching) (Figure 5C). The TU treatment abolishes the increase of

278 *CrCasp8/9* expression (Figure 5C and Table 2). In addition, expression of two key *Bcl2*

279 family (members of the apoptosis intrinsic pathway), *Bax* and *Bcl-XL*, was detected. The

280   expression of *CrBax* mRNA does not change over time, both in control and TU-treated

281   larvae (Figure 5C and Table 2). The expression of *CrBcl-XL* starts to increase 6h post

282   hatching and shows a 5-fold increase 4h later compared to hatching stage but the TU

283   treatment does not alter significantly its expression level (Figure 5C and Table 2). In this

284   context, the molecular mechanism implicated in the tail regression in *Ciona robusta* was

285   investigated by first using specific functional inhibitors of caspases, *i.e.* inhibitors of

286   vertebrate caspase-8 and caspase-9 (IETD-fmk and LEHD-fmk respectively). After 10h of

287   treatment, only 35% of the caspase-9 inhibitor-treated larvae have strong or total tail

288   regression while 70% of untreated larvae no longer have tails (Figure 5B). In contrast, the

289   inhibitor of caspase-8 had no significant influence on tail regression compared to control

290   larvae (Figure 5B).

291

292

4. Discussion

4.1. Thyroid hormone signaling-dependent apoptosis underlies tail regression in Ciona robusta

In amphibians, metamorphic changes involving structural, physiological, biochemical and behavioral transformations are primarily controlled by thyroid hormone signaling and these processes can last for a few several days (Sachs *et al.*, 2000). In ascidians, this process is much faster: Matsunobu and Sasakura have timed the different steps of metamorphosis in *Ciona robusta*, which from hatching to complete tail regression take only 12 hours (Matsunobu & Sasakura, 2015).

After hatching, the progression of an apoptotic wave goes from the posterior to the anterior zone of the *Ciona robusta* tail. Here, we show that the inhibition of T4 signaling by TU blocks the initiation of the apoptotic wave and subsequent tail regression, suggesting that T4 is necessary to initiate apoptosis (Figure 2). This T4 effect, consistent with that found in amphibians (Sachs *et al.*, 1997a; b), is confirmed by the results of our rescue experiments where apoptosis and subsequent tail regression is reactivated by T4 co-treatment with TU (Figure 2).

We show that T4 acts in the initiation of apoptosis *via* activation of an intermediate signaling center located in the tail end. This is congruent with reports of a number of genes being only expressed at the posterior end of the tail of *Ciona robusta* such as *Sccpb* (similar to selectin P), a gene under the MAPK signaling pathway (Cr-ERK and Cr-JNK) that is essential for apoptosis-dependent tail regression (Chambon *et al.*, 2007). Interestingly, ERK is activated by phosphorylation only at the tail end before the wave of apoptosis (Chambon *et al.*, 2002; Krasovec *et al.*, 2019). As a consequence, we postulate that the posterior part of the larval tail contains the signaling source responsible for the initiation of observed wave of apoptosis and the metamorphosis process, and that this signaling center is under the control of T4 signaling. In our tail removal experiments (Figure 3), T4 treatment probably allows local and fast expression/recruitment of proteins specific to the end of tail and then apoptosis recovery at 6hph (Figure 3). Thyroid hormone signaling therefore appears to activate the apoptosis pathway in a directional way in the period preceding adhesion by initiation of the posterior signaling center. The link between thyroid hormone signaling and apoptosis is further documented by the results of qPCR experiments showing a thyroid hormone-dependent transcriptional

12

326   induction of *CrCasp8/9* during tail regression (Figure 5C).

327

328   *4.2. Apoptosis during* Ciona robusta *tail regression does not rely on a classical intrinsic*
329   *pathway*

330   Thyroid hormone-dependent apoptosis in *Xenopus* tadpole involves the intrinsic
331   pathway (Sachs *et al.*, 1997a; b; Xiong *et al.*, 2014; Ichim & Tait, 2016). Our caspase-
332   inhibition treatments support a caspase-9-like activity in the initiation of apoptosis,
333   therefore similar to the function of the intrinsic pathway. However, this experiment
334   cannot identify the exact active caspase involved in the process since the active site of the
335   CrCasp8/9 is comparable to that of human caspase-8 (Figure 5A). Our qPCR results show
336   an important induction of *CrBcl-XL* starting at 6hph, when *CrCasp8/9* mRNA expression is
337   maximal. This result is surprising because the vertebrate Bcl-XL is known for its anti-
338   apoptotic action (for review see (Cui & Placzek, 2018). If this activity is conserved in
339   chordates, the induction of *CrBcl-XL* might have a function in the conservation of an anti-
340   apoptotic state for the cells that migrate to the trunk during tail regression. This is in
341   contrast to the *Xenopus* metamorphosis where Bcl-XL has no apparent function in the
342   thyroid hormone-induced apoptosis (Johnston *et al.*, 2005) and where cell migration from
343   the tail to the body has never been reported (see review Yaoita, 2019).

344

345   *4.3. New model of interaction between thyroid hormone and apoptotic pathway in* Ciona
346   robusta

347   From our results, the interaction between thyroid hormone signaling and the
348   apoptosis in the tail of *Ciona robusta* appears different from that described in *Xenopus*
349   tadpoles. A concomitance between high levels of T4, CrTR and apoptosis is not observed
350   in *Ciona robusta* in contrast to *Xenopus laevis* (Figure 6 according to the work of (Sachs *et*
351   *al.*, 2000; Ishizuya-Oka *et al.*, 2010)). Our results indicate that *CrTR* expression is high at
352   hatching, when *CrRXR* expression and apoptosis are still low or not detected, respectively.
353   After hatching, thyroid hormone and *CrTR* levels progressively decrease concomitantly
354   with increasing quantities of apoptotic nuclei, *CrRXR* and *CrCasp8/9* mRNAs (Figure 6).
355   These results suggest that CrTR behaves like TRα in amphibians where, in the absence of
356   THs, it prevents the progression of metamorphosis and promotes the growth of tadpoles
357   (Wen & Shi, 2015). Transcription of both *CrTR* and *CrRXR* genes is modified by the
358   treatment with TU, arguing for thyroid hormone-dependent expression of both receptors.

13

359 However, the results of these qPCR experiments do not allow to conclude on the
360 functionality of the TR/RXR heterodimer which will require further *in vitro* study of
361 nuclear receptor activities.

362

363 *4.4. Conservation of thyroid hormone and metamorphosis in chordates*

364   Metamorphosis is an ancestral feature of chordates with conserved molecular
365 determinism (Holzer *et al.*, 2017). Thyroid hormones and their receptors have been
366 systematically involved in metamorphosis in all chordates in which their role has been
367 tested, even in animals located at very distant branches of the chordate phylogenetic tree
368 (amphibians, teleost fishes and amphioxus). Different larva-to-juvenile transitions
369 described can be considered as homologous, based on the conservation of the thyroid
370 hormone signaling pathway generated by thyroid hormones and their receptors. We have
371 shown in this study that the thyroid-dependent metamorphosis of *Ciona robusta* has a
372 different mode of operation from what is classically known. Interestingly, another
373 organism also stands out from the other chordates: in the sea lamprey, it is also the drop
374 of circulating T4 that enables its metamorphosis, which shows features of apoptosis in the
375 epithelial cells of the biliary tract (Boomer *et al.*, 2010; Morii *et al.*, 2010) and the
376 pronephric kidney (Ellis & Youson, 1990). But in contrast to *Ciona*, exogenous THs slow
377 down, rather than accelerate, the natural lamprey metamorphosis with binding to their
378 specific receptors (Youson, 1997; Manzon *et al.*, 2014; Manzon & Manzon, 2017) (Figure
379 6). Despite being a more distant vertebrate relative compared to urochordates (Delsuc *et*
380 *al.*, 2006), the amphioxus has a functional thyroid hormone receptor, and THs induce
381 metamorphosis in amphioxus as in the frog, despite apoptosis was not shown during the
382 metamorphic process (Paris *et al.*, 2008). In connection with these comparisons, it is
383 important to note that metamorphosis in *Ciona* lasts only a few hours (instead of several
384 days for the amphioxus, lamprey or xenopus) and in this regard, is more comparable with
385 that of echinoderms within the deuterostomes.

386

387 *4.5. Conservation of thyroid hormone and metamorphosis in bilaterians*

388   Within the deuterostomes, the sea urchin (echinoderm) transforms from a
389 swimming larva into a sessile juvenile (bilateral symmetric larva into radial symmetric
390 and benthonic adult) in a few hours (Sato *et al.*, 2006). All eight arms of the sea urchin
391 larva reduce from their tip to the trunk by apoptosis when treated with THs, and

392   inhibition of apoptosis prevents the induction of metamorphosis (Saito *et al.*, 1998; Lutek
393   *et al.*, 2018; Taylor & Heyland, 2018; Wynen & Heyland, 2021). Similar to *Ciona robusta*,
394   the sea urchin has 1 RXR and 1 TR (Howard-Ashby *et al.*, 2006), exogenous TH treatment
395   accelerates its metamorphosis but transcription of target genes via its TR is not activated
396   by THs (Taylor & Heyland, 2018). Recently, TH action in sea urchin has been shown to act
397   via the MAPK-ERK1/2 pathway (Taylor & Heyland, 2018) as it was shown for *Ciona*
398   *robusta* (Chambon *et al.*, 2007). These similitudes between urochordate and echinoderm
399   metamorphic processes suggest an ancestrally conserved regulation by thyroid hormone,
400   through the MAPK-ERK pathway and involving TR as a constitutive transcriptional
401   regulator, therefore differing significantly from the "classical" vertebrate thyroid
402   hormone signaling.

403   Outside of deuterostomes, in both oysters and mussels, THs peak at the gastrula
404   stage and decrease just after the trochophore stage. This variation is correlated with the
405   presence of the TR (absent after the trochophore stage). The oyster has 1 RXR and 1 TR,
406   and its TR inhibits its own expression supporting the transcriptional repression activity
407   of the TR (Huang *et al.*, 2015). In addition, two caspases play a key role in the loss of the
408   foot and velum during larval metamorphosis (Yang *et al.*, 2015). In mussels, while TH
409   treatment accelerates metamorphosis, knockdown of its TR leads to inhibition of
410   metamorphosis: thus, the TR may have transcriptional repression activity affecting
411   competence for the metamorphic transition (Li *et al.*, 2020) (figure 6). This TH-dependent
412   signaling pathway with TR acting as a constitutive transcription factor may therefore be
413   a probable bilaterian ancestral regulatory pathway. Both this bilaterian and the
414   vertebrate regulatory pathways may have co-existed in the last common ancestor of
415   chordates, and differentially selected for: the "vertebrate"-type was conserved in
416   amphioxus and vertebrates, while the "bilaterian"-type was conserved in *Ciona*
417   (Morthorst *et al.*, 2022).

418

419   **5. Conclusions**

420   Collectively, these results suggest that thyroid hormones are involved in the
421   initiation of the apoptotic wave leading to tail regression in *Ciona robusta,* similar to
422   previous findings in amphibians. However, in *Ciona robusta* the mode of action shows
423   great variation compared to the classically described scheme in vertebrates, both at the
424   level of the thyroid hormone/TR interactions and also at the level of the apoptotic

425   pathway. Despite a phylogenetic position in the vertebrate sister group, *Ciona robusta* has

426   retained the ancestral thyroid hormone pathway, i.e. a non TH/TR interaction but with a

427   constitutive TR that represses progression to metamorphosis by promoting tadpole

428   growth. This significance of the conservation but also these differences might be linked to

429   the evolution of a very rapid metamorphosis in an organism of simple architecture.

430

Acknowledgments

439

Conflicts of interest

441   The authors declare that there is no conflict of interest that could be perceived as

442   prejudicing the impartiality of the research reported.

443

Ethical approval

445   The research described herein was performed on *Ciona robusta*, a marine invertebrate.

446   The study was carried out in strict accordance with European and French legislations

447   (directives 2010/63 and 2016-XIX-120, respectively) for the care and use of animals for

448   scientific purposes (ISEM agreement N°A34-172-042) although *Ciona robusta* is not

449   included in the organisms designated by this legislation. The study did not involve

450   endangered nor protected species.

451

References

452   **References**

453 Barrington, E.J. & Thorpe, A. 1965. The identification of monoiodotyrosine, diiodotyrosine
454 and thyroxine in extracts of the endostyle of the ascidian, Ciona intestinalis L. *Proceedings of*
455 *the Royal Society of London. Series B, Biological sciences* **163**: 136–49.

456 Boomer, L.A., Bellister, S.A., Stephenson, L.L., Hillyard, S.D., Khoury, J.D., Youson, J.H.,
457 *et al.* 2010. Cholangiocyte apoptosis is an early event during induced metamorphosis in the
458 sea lamprey, Petromyzon marinus L. *Journal of Pediatric Surgery* **45**: 114–120.

459 Brunetti, R., Gissi, C., Pennati, R., Caicci, F., Gasparini, F. & Manni, L. 2015. Morphological
460 evidence that the molecularly determined Ciona intestinalis type A and type B are different
461 species: Ciona robusta and Ciona intestinalis. *Journal of Zoological Systematics and*
462 *Evolutionary Research* **53**: 186–193.

463 Carosa, E., Fanelli, A., Ulisse, S., Di Lauro, R., Rall, J.E. & Jannini, E.A. 1998. *Ciona*
464 *intestinalis* nuclear receptor 1: A member of steroid/thyroid hormone receptor family. *Proc.*
465 *Natl. Acad. Sci. U.S.A.* **95**: 11152–11157.

466 Chambon, J.-P., Nakayama, A., Takamura, K., McDougall, A. & Satoh, N. 2007. ERK- and
467 JNK-signalling regulate gene networks that stimulate metamorphosis and apoptosis in tail
468 tissues of ascidian tadpoles. *Development* **134**: 1203–1219.

469 Chambon, J.-P., Soule, J., Pomies, P., Fort, P., Sahuquet, A., Alexandre, D., *et al.* 2002. Tail
470 regression in *Ciona intestinalis* (Prochordate) involves a Caspase-dependent apoptosis event
471 associated with ERK activation. *Development* **129**: 3105–3114.

472 Cui, J. & Placzek, W.J. 2018. Post-Transcriptional Regulation of Anti-Apoptotic BCL2
473 Family Members. *International Journal of Molecular Sciences* **19**: 308.

474 D'Agati, P. & Cammarata, M. 2006. Comparative analysis of thyroxine distribution in
475 ascidian larvae. *Cell and Tissue Research* **323**: 529–535.

476 Dehal, P., Satou, Y., Campbell, R.K., Chapman, J., Degnan, B., De Tomaso, A., *et al.* 2002.
477 The Draft Genome of *Ciona intestinalis* : Insights into Chordate and Vertebrate Origins.
478 *Science* **298**: 2157–2167.

479 Delsuc, F., Brinkmann, H., Chourrout, D. & Philippe, H. 2006. Tunicates and not
480 cephalochordates are the closest living relatives of vertebrates. *Nature* **439**: 965–968.

481 Di Fiore, M.M., Perrone, L. & D'Aniello, A. 1997. Presence of a human-like thyroid
482 stimulating hormone (TSH) in Ciona intestinalis. *Life Sciences* **61**: 623–629.

483 Dunn, A.D. 1980a. Properties of an iodinating enzyme in the ascidian endostyle. *General and*
484 *Comparative Endocrinology* **40**: 484–493.

485 Dunn, D. 1980b. Studies on lodoproteins avd Thyroid Hormones in Ascidians. 473–483.

486 Ellis, L.C. & Youson, J.H. 1990. Pronephric regression during larval life in the sea lamprey,
487 Petromyzon marinus L.: A histochemical and ultrastructural study. *Anat Embryol* **182**.

488 Fujita, H. & Sawano, F. 1979. Fine structural localization of endogeneous peroxidase in the
489 endostyle of ascidians, Ciona intestinalis. A part of phylogenetic studies of the thyroid gland.
490 *Archivum histologicum Japonicum = Nihon soshikigaku kiroku* **42**: 319–26.

491 Goemann, I.M., Romitti, M., Meyer, E.L.S., Wajner, S.M. & Maia, A.L. 2017. Role of
492 thyroid hormones in the neoplastic process: an overview. *Endocrine-related cancer* **24**:
493 R367–R385.

494 Grimaldi, A.G., Buisine, N., Bilesimo, P. & Sachs, L.M. 2013. High-Throughput Sequencing
495 Will Metamorphose the Analysis of Thyroid Hormone Receptor Function During Amphibian
496 Development. *Current Topics in Developmental Biology* **103**: 277–303.

497 Hanada, H., Kobuchi, H., Yamamoto, M., Kashiwagi, K., Katsu, K., Utsumi, T., *et al.* 2013.
498 Acetyl-L-carnitine suppresses thyroid hormone-induced and spontaneous anuran tadpole tail
499 shortening. *Hereditas* **150**: 1–9.

500 Holzer, G. & Laudet, V. 2013. Chapter Fourteen - Thyroid Hormones and Postembryonic
501 Development in Amniotes. *Animal Metamorphosis* **Volume 103**: 397–425.

502 Holzer, G., Roux, N. & Laudet, V. 2017. Evolution of ligands, receptors and metabolizing
503 enzymes of thyroid signaling. *Molecular and Cellular Endocrinology* 1–9. Elsevier Ireland
504 Ltd.

505 Hotta, K., Dauga, D. & Manni, L. 2020. The ontology of the anatomy and development of the
506 solitary ascidian Ciona: the swimming larva and its metamorphosis. *Sci Rep* **10**: 17916.

507 Howard-Ashby, M., Materna, S.C., Brown, C.T., Chen, L., Cameron, R.A. & Davidson, E.H.
508 2006. Gene families encoding transcription factors expressed in early development of
509 Strongylocentrotus purpuratus. *Developmental Biology* **300**: 90–107.

510 Huang, W., Xu, F., Qu, T., Zhang, R., Li, L., Que, H., *et al.* 2015. Identification of Thyroid
511 Hormones and Functional Characterization of Thyroid Hormone Receptor in the Pacific
512 Oyster Crassostrea gigas Provide Insight into Evolution of the Thyroid Hormone System.
513 *PLoS ONE* **10**: e0144991.

514 Ichim, G. & Tait, S.W.G. 2016. A fate worse than death: apoptosis as an oncogenic process.
515 *Nat Rev Cancer* **16**: 539–548.

516 Ikeda, M., Rhee, M. & Chin, W.W. 1994. Thyroid hormone receptor monomer, homodimer,
517 and heterodimer (with retinoid-X receptor) contact different nucleotide sequences in thyroid
518 hormone response elements. *Endocrinology* **135**: 1628–1638.

519 Ishizuya-Oka, A. 2011. Amphibian organ remodeling during metamorphosis: Insight into
520 thyroid hormone-induced apoptosis. *Development Growth and Differentiation* **53**: 202–212.

521 Ishizuya-Oka, A., Hasebe, T. & Shi, Y.B. 2010. Apoptosis in amphibian organs during
522 metamorphosis. *Apoptosis* **15**: 350–364.

523 Johnston, J., Chan, R., Calderon-Segura, M., McFarlane, S. & Browder, L.W. 2005. The roles
524 of Bcl-xL in modulating apoptosis during development of Xenopus laevis. *BMC*
525 *developmental biology* **5**: 20.

526 Karaiskou, A., Swalla, B.J., Sasakura, Y. & Chambon, J.P. 2015. Metamorphosis in solitary
527 ascidians. *Genesis* **53**: 34–47.

528 Krasovec, G., Robine, K., Quéinnec, E., Karaiskou, A. & Chambon, J.P. 2019. Ci-hox12 tail
529 gradient precedes and participates in the control of the apoptotic-dependent tail regression
530 during Ciona larva metamorphosis. *Developmental Biology* **448**: 237–246.

531 Li, Y.-F., Cheng, Y.-L., Chen, K., Cheng, Z.-Y., Zhu, X., C. R. Cardoso, J., *et al.* 2020.
532 Thyroid hormone receptor: A new player in epinephrine-induced larval metamorphosis of the
533 hard-shelled mussel. *General and Comparative Endocrinology* **287**: 113347.

534 Lutek, K., Dhaliwal, R.S., Van Raay, T.J. & Heyland, A. 2018. Sea urchin histamine receptor
535 1 regulates programmed cell death in larval Strongylocentrotus purpuratus. *Sci Rep* **8**: 4002.

536 Machado, D.S., Sabet, A., Santiago, L.A., Sidhaye, A.R., Chiamolera, M.I., Ortiga-Carvalho,
537 T.M., *et al.* 2009. A thyroid hormone receptor mutation that dissociates thyroid hormone
538 regulation of gene expression in vivo. *Proceedings of the National Academy of Sciences* **106**:
539 9441–9446.

540 Manzon, L.A., Youson, J.H., Holzer, G., Staiano, L., Laudet, V. & Manzon, R.G. 2014.
541 Thyroid hormone and retinoid X receptor function and expression during sea lamprey
542 (Petromyzon marinus) metamorphosis. *General and Comparative Endocrinology* **204**: 211–
543 222.

544 Manzon, R.G. & Manzon, L.A. 2017. Lamprey metamorphosis: Thyroid hormone signaling in
545 a basal vertebrate. *Molecular and Cellular Endocrinology* **459**: 28–42.

546 Matsunobu, S. & Sasakura, Y. 2015. Time course for tail regression during metamorphosis of
547 the ascidian Ciona intestinalis. *Developmental Biology* **405**: 71–81. Elsevier.

548 Morii, M., Mezaki, Y., Yamaguchi, N., Yoshikawa, K., Miura, M., Imai, K., *et al.* 2010.
549 Onset of Apoptosis in the Cystic Duct During Metamorphosis of a Japanese Lamprey,
550 Lethenteron reissneri. *Anat Rec* **293**: 1155–1166.

551 Morthorst, J.E., Holbech, H., De Crozé, N., Matthiessen, P. & LeBlanc, G.A. 2022. Thyroid-
552 like hormone signaling in invertebrates and its potential role in initial screening of thyroid
553 hormone system disrupting chemicals. *Integr Envir Assess & Manag* ieam.4632.

554 Morvan-Dubois, G., Fini, J.B. & Demeneix, B.A. 2013. *Is Thyroid Hormone Signaling
555 Relevant for Vertebrate Embryogenesis?*

556 Mullur, R., Liu, Y.-Y. & Brent, G.A. 2014. Thyroid Hormone Regulation of Metabolism.
557 *Physiological Reviews* **94**: 355–382.

558 Ogasawara, M., Di Lauro, R. & Satoh, N. 1999. Ascidian homologs of mammalian thyroid
559 peroxidase genes are expressed in the thyroid-equivalent region of the endostyle. *The Journal
560 of experimental zoology* **285**: 158–69.

561 Paris, M., Escriva, H., Schubert, M., Brunet, F., Brtko, J., Ciesielski, F., *et al.* 2008.
562 Amphioxus Postembryonic Development Reveals the Homology of Chordate Metamorphosis.
563 *Current Biology* **18**: 825–830.

564 Patricolo, E., Cammarata, M. & Dagati, P. 2001. Presence of thyroid hormones in ascidian
565 larvae and their involvement in metamorphosis. *Journal of Experimental Zoology* **290**: 426–
566 430.

567 Roche, J., Salvatore, G. & Giuseppe, E.T. 1962. Jean roche, gaetano salvatore et giuseppe
568 rametta. **63**.

569 Rowe, I., Le Blay, K., Du Pasquier, D., Palmier, K., Levi, G., Demeneix, B., *et al.* 2005.
570 Apoptosis of tail muscle during amphibian metamorphosis involves a caspase 9-dependent

571 mechanism. *Developmental Dynamics* **233**: 76–87.

572 Sachs, L.M., Abdallah, B., Hassan, A., Levi, G., De Luze, A., Reed, J.C., *et al.* 1997a.
573 Apoptosis in *Xenopus* tadpole tail muscles involves Bax-dependent pathways. *FASEB j.* **11**:
574 801–808.

575 Sachs, L.M., Damjanovski, S., Jones, P.L., Li, Q., Amano, T., Ueda, S., *et al.* 2000. Dual
576 functions of thyroid hormone receptors during Xenopus development. *Comparative*
577 *biochemistry and physiology. Part B, Biochemistry & molecular biology* **126**: 199–211.

578 Sachs, L.M., Le Mevel, S. & Demeneix, B.A. 2004. Implication of bax in Xenopus laevis tail
579 regression at metamorphosis. *Developmental Dynamics* **231**: 671–682.

580 Sachs, L.M., Lebrun, J.J., de Luze, A., Kelly, P.A. & Demeneix, B.A. 1997b. Tail regression,
581 apoptosis and thyroid hormone regulation of myosin heavy chain isoforms in Xenopus
582 tadpoles. *Molecular and Cellular Endocrinology* **131**: 211–219.

583 Saito, M., Seki, M., Amemiya, S., Yamasu, K., Suyemitsu, T. & Ishihara, K. 1998. Induction
584 of metamorphosis in the sand dollar Peronella japonica by thyroid hormones. *Dev Growth*
585 *Differ* **40**: 307–312.

586 Sasakura, Y. & Hozumi, A. 2017. Formation of adult organs through metamorphosis in
587 ascidians. *Wiley Interdisciplinary Reviews: Developmental Biology* **1**.

588 Sato, Y., Kaneko, H., Negishi, S. & Yazaki, I. 2006. Larval arm resorption proceeds
589 concomitantly with programmed cell death during metamorphosis of the sea urchin
590 Hemicentrotus pulcherrimus. *Cell Tissue Res* **326**: 851–860.

591 Seoane-Collazo, P., Fernø, J., Gonzalez, F., Diéguez, C., Leis, R., Nogueiras, R., *et al.* 2015.
592 Hypothalamic-autonomic control of energy homeostasis. *Endocrine* **50**: 276–91.

593 Shi, Y.B. & Ishizuya-Oka, A. 2001. Thyroid hormone regulation of apoptotic tissue
594 remodeling: implications from molecular analysis of amphibian metamorphosis. *Progress in*
595 *nucleic acid research and molecular biology* **65**: 53–100.

596 Tarallo, R. & Sordino, P. 2004. Time course of programmed cell death inCiona intestinalis in
597 relation to mitotic activity and MAPK signaling. *Dev. Dyn.* **230**: 251–262.

598 Tata, J.R. 2006. Amphibian metamorphosis as a model for the developmental actions of
599 thyroid hormone. *Molecular and Cellular Endocrinology* **246**: 10–20.

600 Taylor, E. & Heyland, A. 2018. Thyroid Hormones Accelerate Initiation of Skeletogenesis via
601 MAPK (ERK1/2) in Larval Sea Urchins (Strongylocentrotus purpuratus). *Front. Endocrinol.*
602 **9**: 439.

603 Terajima, D., Shida, K., Takada, N., Kasuya, A., Rokhsar, D., Satoh, N., *et al.* 2003.
604 Identification of candidate genes encoding the core components of the cell death machinery in
605 the Ciona intestinalis genome. *Cell Death Differ* **10**: 749–753.

606 Vincent, S., Marty, L. & Fort, P. 1993. S26 ribosomal protein RNA: an invariant control for
607 gene regulation experiments in eucaryotic cells and tissues. *Nucleic acids research* **21**: 1498.

608 Weill, M., Philips, A., Chourrout, D. & Fort, P. 2005. The caspase family in urochordates:
609 distinct evolutionary fates in ascidians and larvaceans. *Biology of the Cell* **97**: 857–866.

610 Wen, L. & Shi, Y.-B. 2015. Unliganded Thyroid Hormone Receptor α Controls
611 Developmental Timing in Xenopus tropicalis. *Endocrinology* **156**: 721–734.

612 Wrutniak-Cabello, C., Casas, F. & Cabello, G. 2017. Mitochondrial T3 receptor and targets.
613 *Molecular and Cellular Endocrinology* **458**: 112–120.

614 Wynen, H. & Heyland, A. 2021. Hormonal Regulation of Programmed Cell Death in Sea
615 Urchin Metamorphosis. *Front. Ecol. Evol.* **9**: 733787.

616 Xiong, S., Mu, T., Wang, G. & Jiang, X. 2014. Mitochondria-mediated apoptosis in
617 mammals. *Protein Cell* **5**: 737–749.

618 Yagi, K., Satou, Y., Mazet, F., Shimeld, S.M., Degnan, B., Rokhsar, D., *et al.* 2003. A
619 genomewide survey of developmentally relevant genes in Ciona intestinalis. III. Genes for
620 Fox, ETS, nuclear receptors and NFKB. *Development Genes and Evolution* **213**: 235–244.

621 Yang, B., Li, L., Pu, F., You, W., Huang, H. & Ke, C. 2015. Molecular cloning of two
622 molluscan caspases and gene functional analysis during Crassostrea angulata (Fujian oyster)
623 larval metamorphosis. *Mol Biol Rep* **42**: 963–975.

624 Yaoita, Y. 2019. Tail Resorption During Metamorphosis in Xenopus Tadpoles. *Front.*
625 *Endocrinol.* **10**: 143.

626 Youson, J.H. 1997. Is Lamprey Metamorphosis Regulated by Thyroid Hormones? *Am Zool*
627 **37**: 441–460.

628

629 **Table 1: Forward and reverse primers used for qPCR experiments**

630

Name (fragment size)	Forward primer	Reverse primer
CrTR (227 bp) KH2012:KH.C11.612	CCCGACGATCATACACCTCT	GACCACACACCGTAATGCTG
CrRXR (220 bp) KH2012:KH.C9.892	GTTCTGAGGCCCCTACTGTT	TGTGGGTACTGGAGTGGAAC
CrCasp8/9 (204 bp) KH2012:KH.C8.550	ATGCATGGAGGAGGAAGACC	CGTTGCGTCAGGGTTTAACTC
CrBax (242 bp) KH2012:KH.C4.794	AGAGAACAGCCCAGTTGAGC	CCCAATTGAAGTTGCCGTCC
CrBcl-XL (185 bp) KH2012:KH.S653.2	GCGGCAGAATACGAGAGAAG	GAGTTGCTGGTTGCTTGTGA
CrS26 (162 bp) KH2012:KH.C2.257	AAGGACGCGGTCATGTAAAA	TCTTTGGCAAGGCGTAAGAT

631

632 **Table 2: Analysis of Variance (ANOVA) for qPCR experiments. Bold numbers mean**

633 *P* **value < 0.05**

gene	Predictor	Sum Sq	Mean Sq	F value	Pr(>F)
CrCasp8/9	time	0.5663	0.5663	1.5028	0.229180
	treatment	4.4219	4.4219	11.7347	**0.001702**
	time:treatment	0.5527	0.5527	1.4668	0.234726
CrBax	time	0.9929	0.99294	4.0365	0.05302
	treatment	0.2244	0.22439	0.9122	0.34669
	time:treatment	0.0580	0.05801	0.2358	0.63055
CrBclXl	time	53.444	53.444	39.1998	**5.11e-07**
	treatment	3.867	3.867	2.8363	0.1019
	time:treatment	3.478	3.478	2.5509	0.1201
CrRXR	time	17.797	17.7974	16.1577	**0.0003314**
	treatment	5.245	5.2449	4.7617	**0.0365539**
	time:treatment	0.053	0.0527	0.0479	0.8282364
CrTR	time	1612.47	1612.47	87.8360	**8.037e-10**
	treatment	372.28	372.28	20.2793	**0.0001247**
	time:treatment	0.25	0.25	0.0138	0.9074141

634

635 **Legends of figures**

636

637 **Figure 1: T4 disappearance, *CrTR* expression decrease and apoptosis wave in the**

638 **tail of *Ciona robusta*.**

639 A: TUNEL detection (red nuclei) and T4 immunostaining (green) at different stages of

640 development (hph: hour post-hatching) by confocal microscopy. The kinetic was repeated

641 three times and representative images are shown. Scale bar: 100µm. B and C: time course

642 of thyroid hormone receptor *CrTR* mRNA expression between 0 to 28hpf of *Ciona robusta*

643 development (semi quantitative PCR). The extent of *CrTR* expression was compared with

644 *CrS26* mRNA. B: a representative gel agarose image; C: the corresponding histogram is the

645 mean of three independent experiments with standard deviation. The value set to 1 was

646 chosen as the mean value at 18 hpf. The * represents the *P* value between 18hpf and the

647 other time points with *P*<0.05.

648

649 **Figure 2: Inhibition of metamorphosis by thiourea (TU) and rescue with T4**

650 **treatment.**

651 Hatching larvae were treated (TU) or not (control) with TU 500µM and collected after 6h

652 and 12h of treatment. Rescue larvae (TU+T4) were treated at hatching time with TU

653 500µM/T4 100nM mixture and collected at 6h and 12h of treatment. Fixed larvae were

654 double-labeled with TUNEL (red) and Dapi (blue) and observed by confocal microscopy.

655 The double labeling is shown with the tail contour drawn in grey. The experiment was

656 repeated three times and percentage of larvae showing the presented expression pattern

657 is indicated on each panel. Scale bar: 100µm except for 12hph Control (75µm).

658

659 **Figure 3: Metamorphosis of amputated larvae treated with T4**

660 At hatching, the posterior extremity of larva tails (a quarter) was removed, amputated

661 larvae were treated or not with T4 100nM and collected at 6h and 12h of treatment. For

662 each kinetic point, state of 50 larvae was counted (metamorphosed *versus* swimming

663 larvae), then collected and fixed for apoptosis detection (TUNEL, white nuclei). A: The

664 histograms are the mean of three independent experiments with standard deviation. The

665 * represents the *P* value between untreated and T4 treated larvae with *P*<0.05. Cont Swim:

666 swimming untreated larvae; Cont Met: metamorphosed untreated larvae; T4 Swim:

667 swimming T4 treated larvae; T4 Met: metamorphosed T4 treated larvae. B-C:

24

668   Representative images for apoptosis detection in untreated (B) and T4 treated (C)

669   amputated larvae are shown at 12 and 6hph, respectively. Percentage of larvae showing

670   the presented expression pattern is indicated on each panel. Scale bar: 100μm (insert

671   scale bar: 30μm)

672

673   **Figure 4: mRNA expression of *CrTR* and *CrRXR* during metamorphosis**

674   Time course of *CrTR* (A) and *CrRXR* (B) mRNA expression from hatching to 10hph in

675   control (dark grey) and TU treated (light grey) tails by qPCR. The histograms are the mean

676   of three independent experiments (*i.e.* 3 different spawns with each time point

677   corresponding to a pool of larvae) with standard deviation; data were normalized to

678   respective *CrS26* mRNA expression values. A relative mRNA quantity value of one

679   corresponds to the lowest amount of control target mRNA. The * represents the *P* value

680   between control and TU treated larvae at the same stage with P<0.05. The a and b

681   represent the *P* value between hatching and the different stages in control and TU treated

682   larvae, respectively, with *P*<0.05.

683

684   **Figure 5: Detection of intrinsic apoptosis during metamorphosis of *Ciona robusta***

685   A: Schematic representation of CrCasp8/9 compared with human caspases -8 and -9 by

686   sequence homology. B: Activity of specific caspase inhibitors. At hatching, larvae were

687   treated with control (DMSO), 100 μM IETD-fmk (caspase-8 inhibitor) or 100 μM LEHD-

688   fmk (caspase-9 inhibitor). Tail regression was evaluated 10h after treatment. "Strong

689   regression" corresponds to a regression of 50 % of the tail or more (light grey) and "Weak

690   regression" corresponds to a decrease of less than 50% of the tail (dark grey). The

691   histograms are the mean of two independent experiments; for each treatment, state of

692   100 larvae was counted. C: Time course of mRNA expression of *CrCasp8/9*, *CrBax* and

693   *CrBcl-XL* from hatching to metamorphosis (hph) in control (dark grey) and TU treated

694   (light grey) tails. The histograms are the mean of three independent experiments (*i.e.* 3

695   different spawns with each time point corresponding to a pool of larvae) with standard

696   deviation; data were normalized to respective *CrS26* mRNA expression values. A relative

697   mRNA quantity value of one corresponds to the amount of target mRNA at hatching time.

698   The * represents the *P* value with *P*<0.05. The a represents the *P* value between hatching

699   and the different stages in control with *P*<0.05.

700

701 **Figure 6: Comparative scheme between *Xenopus* and *Ciona robusta* tadpole**

702 **metamorphoses**

703 Summary of developmental stage-dependent expression of TR and RXR genes and tail cell

704 death of *Ciona robusta* tadpole (A) in comparison to *Xenopus* tadpole (B) during

705 metamorphosis. preM and proM, pre- and prometamorphosis, respectively (adapted from

706 (Sachs *et al.*, 2000; Rowe *et al.*, 2005; Ishizuya-Oka *et al.*, 2010; Matsunobu & Sasakura,

707 2015; Hotta *et al.*, 2020).

708

709 **Supplementary data:**

710 T4 staining (white) at different stages of development, from hatching to the end of tail

711 regression (hph: hour post-hatching) by confocal microscopy. The kinetic was repeated

712 three times and representative images are shown. Scale bar: 100μm except for late tail

713 regression at 30hph (25μm).

714

715   Figure 1

716
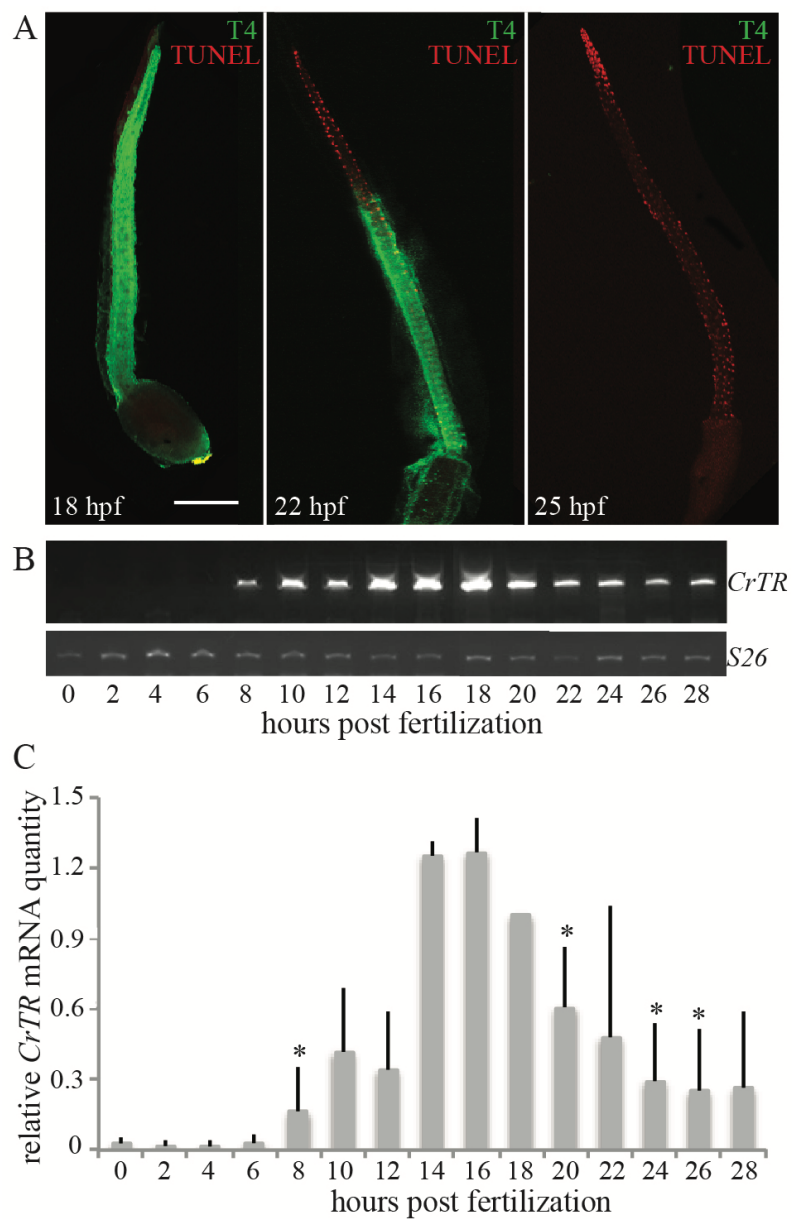
717

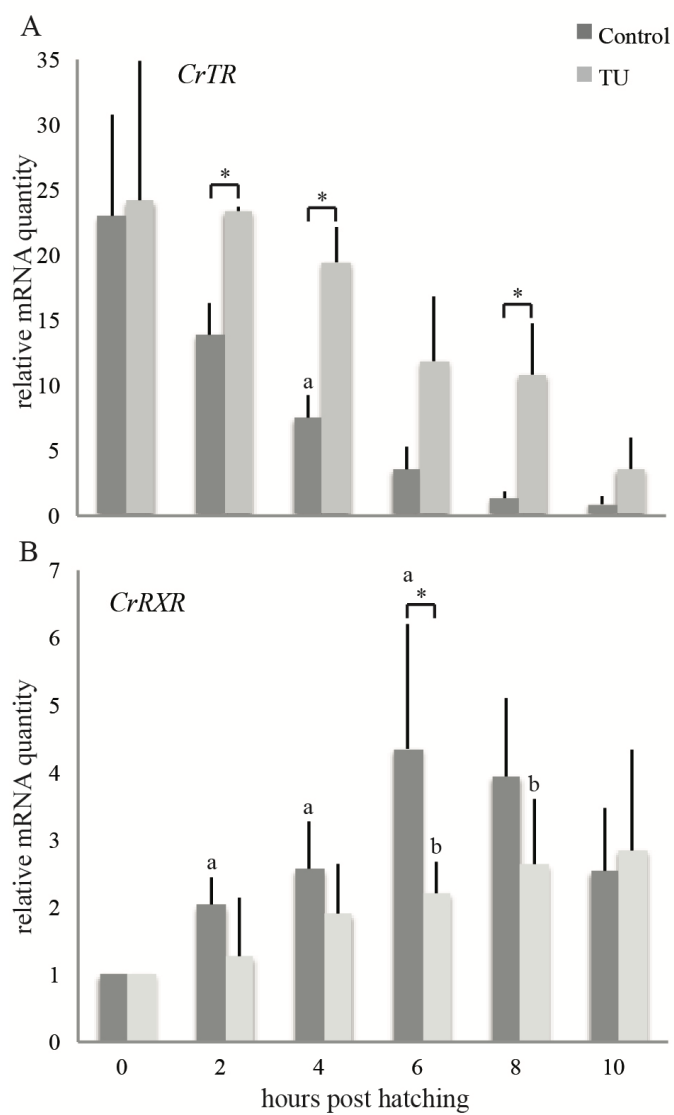718   Figure 2

719
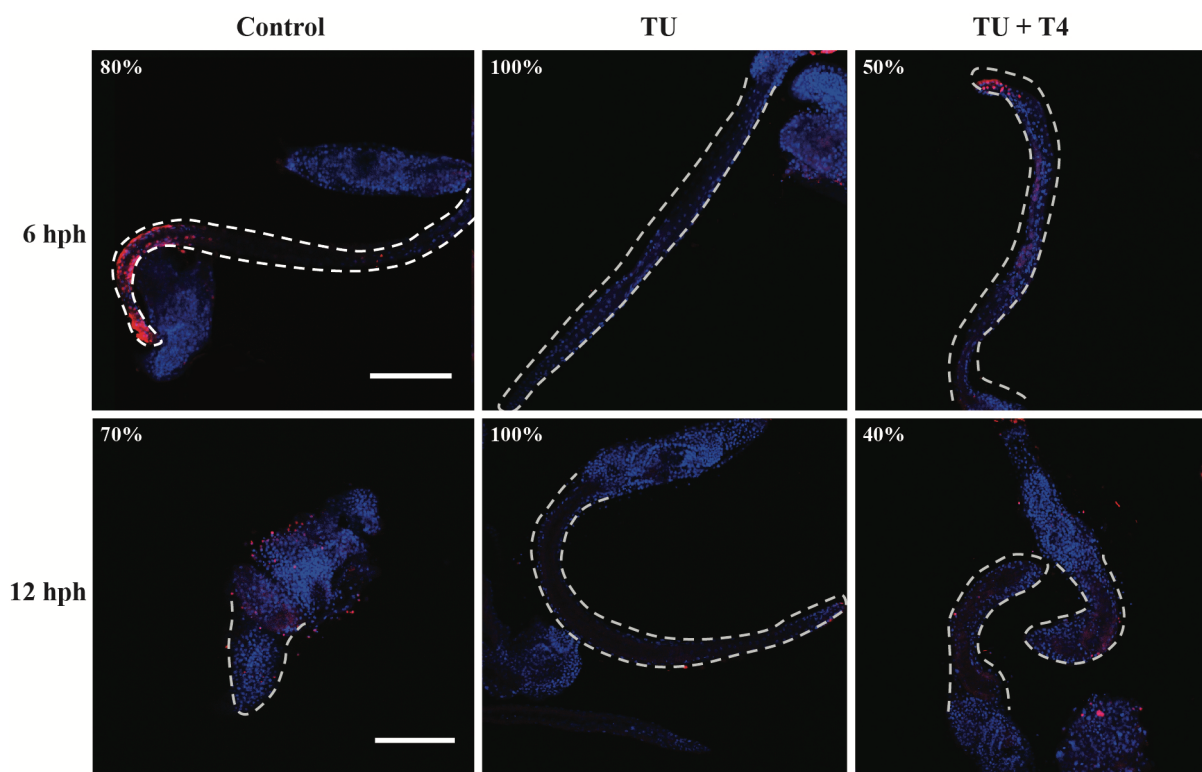
720

721
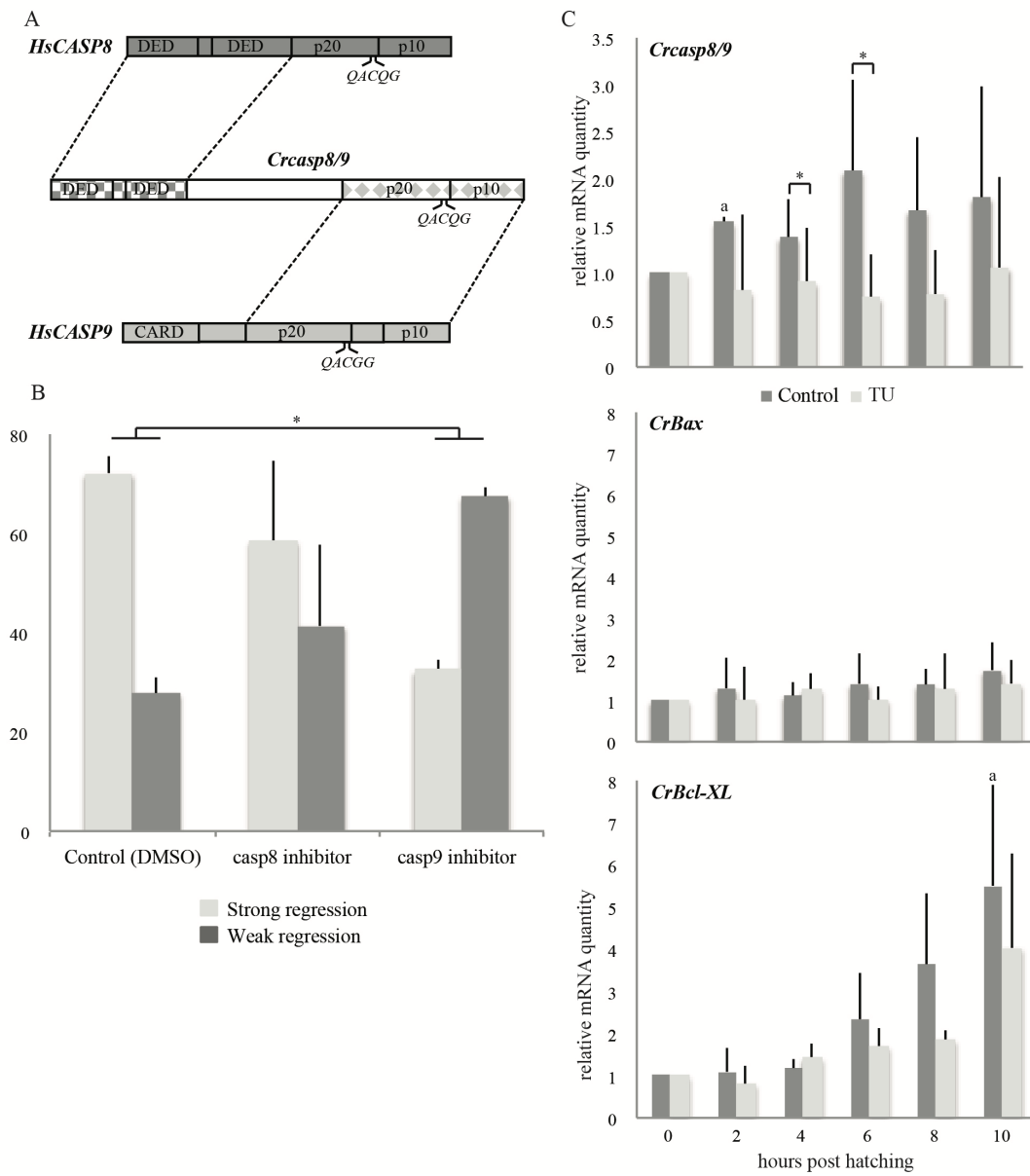
722   Figure 3

723
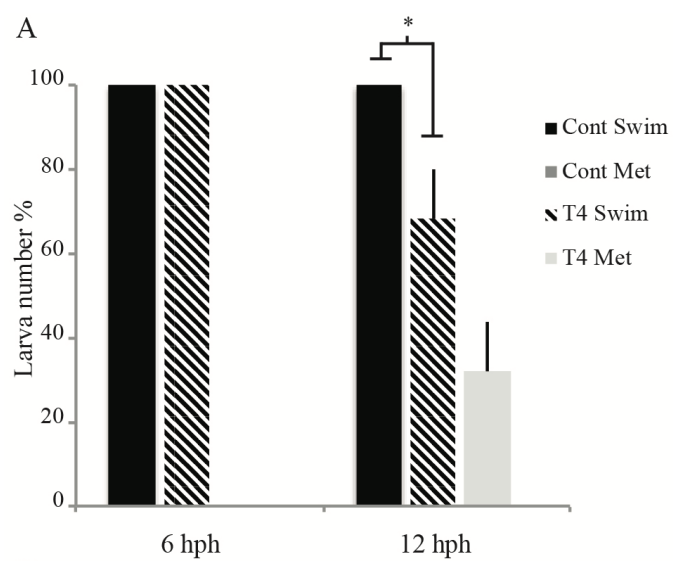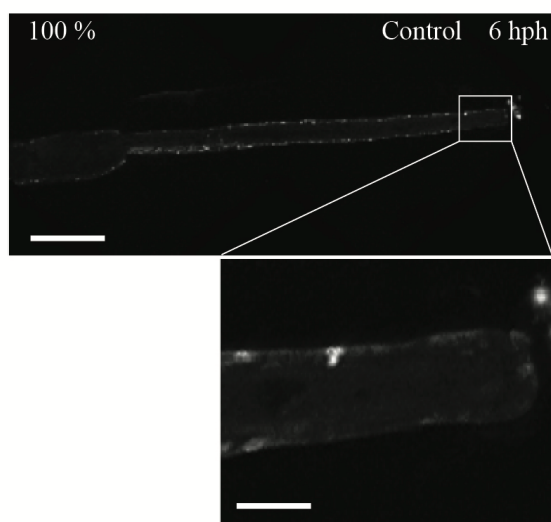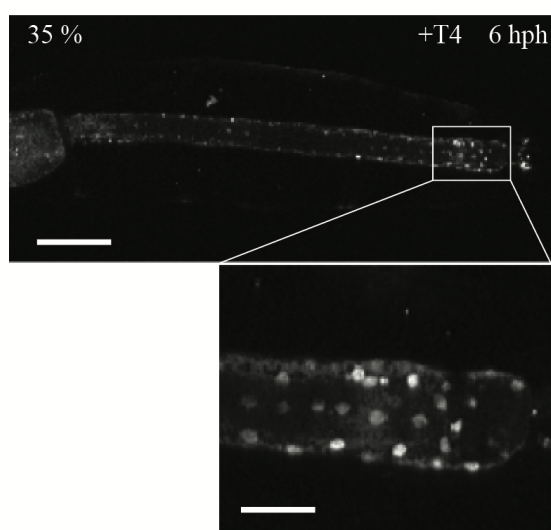
724

725

726   Figure 4

727

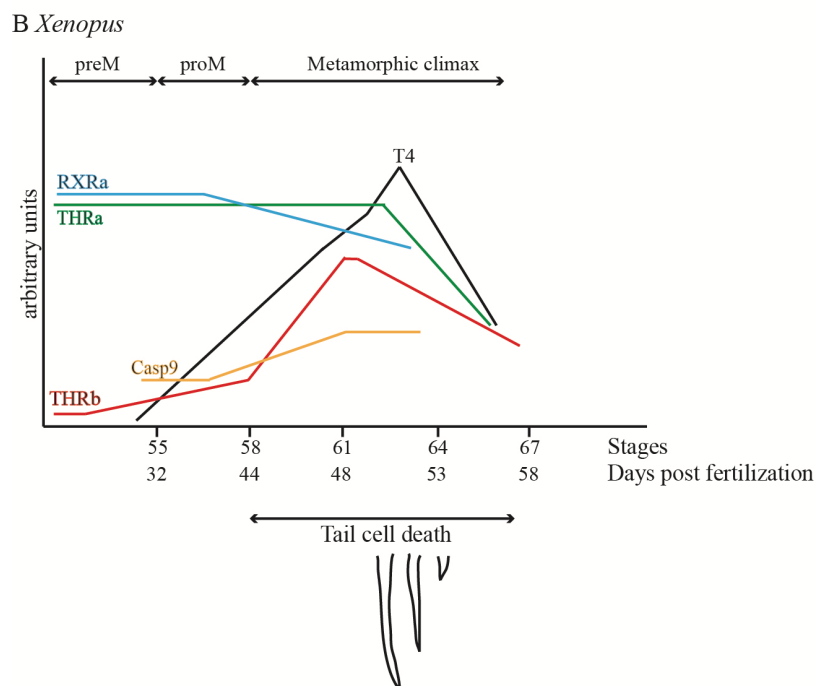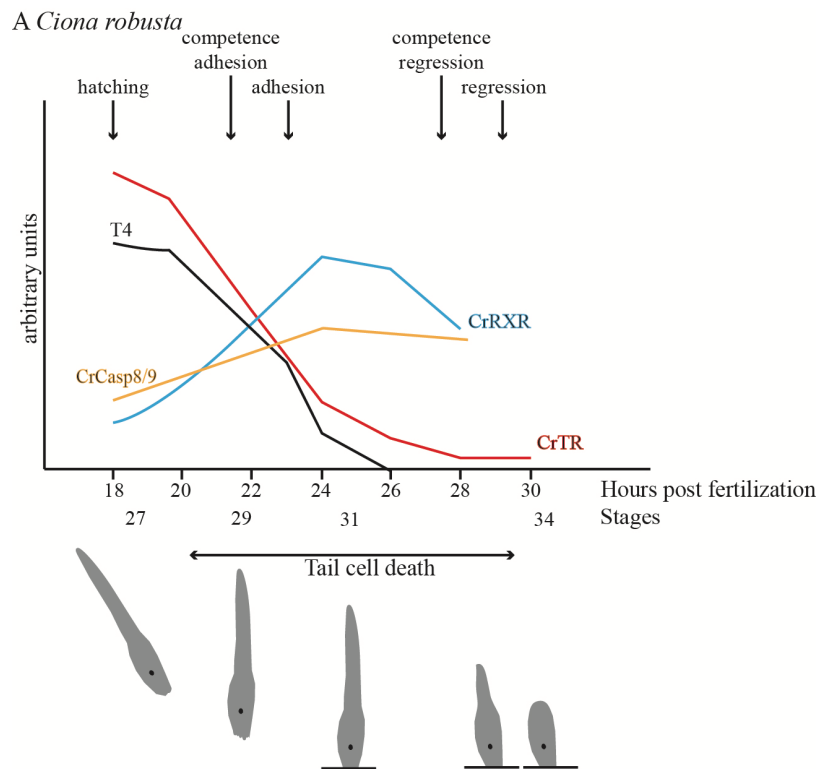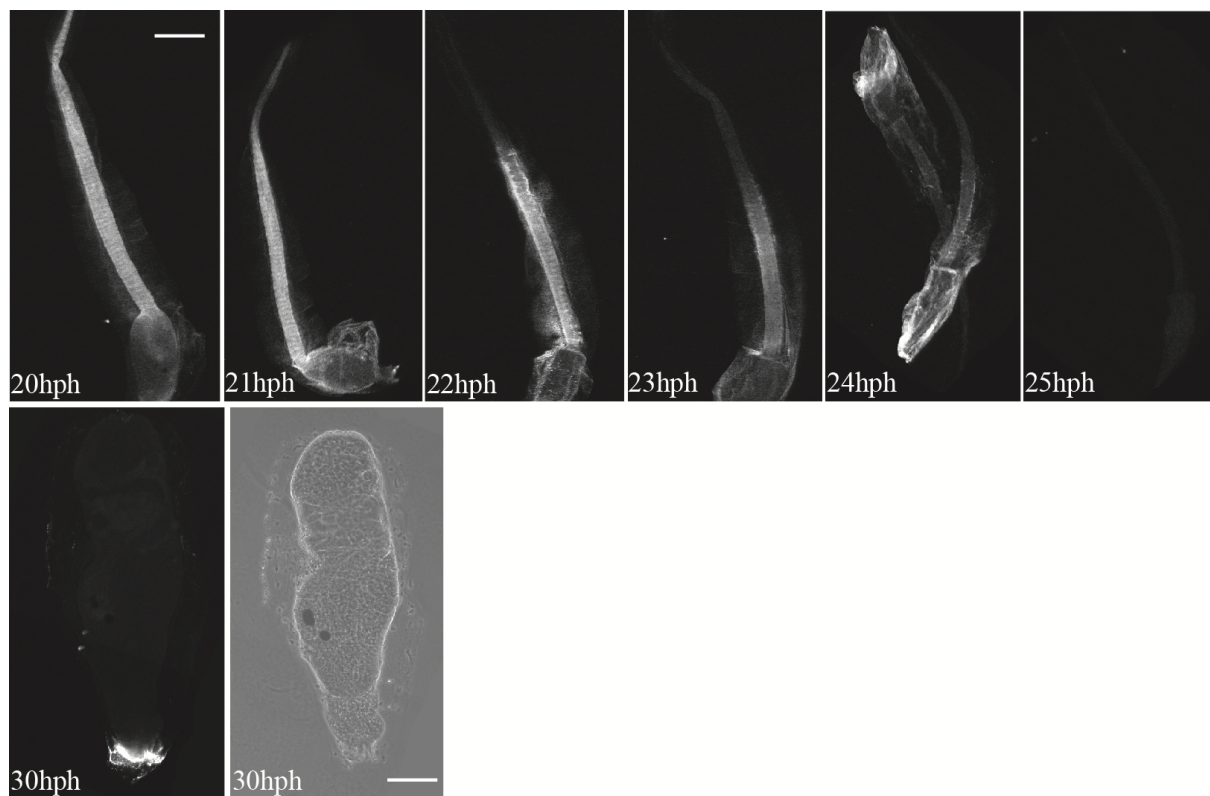728

729

730   Figure 5

731

732
733

734   Figure 6

735

736

737

738   Supplementary data

739

740